J. Fluid Mech. (2001), *vol.* 428, *pp.* 61–80. Printed in the United Kingdom

Rapidly rotating thermal convection at low Prandtl number

By J. H. P. DAWES

Department of Applied Mathematics and Theoretical Physics, University of Cambridge, Silver Street, Cambridge, CB3 9EW, UK

(Received 17 January 2000 and in revised form 10 August 2000)

Rotating Boussinesq convection in a plane layer is governed by two dimensionless groups in addition to the Rayleigh number R: the Prandtl number σ and the Taylor number Ta. Scaled equations for fully nonlinear rotating convection in the limit of rapid rotation and small Prandtl number, where the onset of convection is oscillatory, are derived by considering distinguished limits where $\sigma^n Ta^{1/2} \sim 1$ but $\sigma \to 0$ and $Ta \to \infty$, for different $n > 1$. In the resulting asymptotic expansion in powers of $Ta^{-1/2}$ the leading-order equations, which are independent of n, are solved to provide an analytic description of fully nonlinear convection. Three distinct asymptotic regimes are identified, distinguished by the relative importance of the subdominant buoyancy and inertial terms. For the most interesting case, $n = 4$, the stability of different planforms near onset is investigated using a double expansion in powers of $Ta^{-1/8}$ and the amplitude of convection ε. The lack of a buoyancy term at leading order demands that the perturbation expansion be continued through six orders to derive amplitude equations determining the dynamics. The case $n = 1$ is also analysed. The relevance of this theory to experimental results is briefly discussed.

1. Introduction

Rotating thermal convection is a process of great geophysical and astrophysical importance. Even in idealized settings, solving the equations of motion is a complex task usually attempted either numerically or by an expansion in terms of a small parameter, for example the amplitude of the convective motion. Low Prandtl number convection is particularly relevant to some astrophysical situations: these may involve fluids with Prandtl numbers as low as 10^{-8}. It is also relevant to convection in liquid metals, where typical Prandtl numbers are in the range 10^{-3} to 10^{-2}. Asymptotic analyses of non-rotating convection in the limit of small σ have been performed by Proctor (1977) and Busse & Clever (1981) in response to the two-dimensional numerical simulations of Jones, Moore & Weiss (1976) and Clever & Busse (1981). The motion is dominated by inertial forces, and the analytic results agree well with the experimental results on non-rotating convection in mercury ($\sigma \approx 0.025$) obtained by Rossby (1969). The analysis of Proctor (1977) shows a second feature of non-rotating low Prandtl number convection which has been confirmed by experimental results (Kek & Müller 1993): the Nusselt number increases very little above the critical Rayleigh number R_c for the onset of convection until a second critical Rayleigh number $R_2 > R_c$ (Busse & Clever 1981) is reached. For $R > R_2$ the heat transfer increases much more rapidly; there is a break in the slope of the Nu–R curve.

Convection in the limit of rapid rotation (with $\sigma \sim 1$) has been investigated by many authors: Chandrasekhar (1961) noted the scalings of the critical wavenumber and Rayleigh number for the onset of convection when the Taylor number (the non-dimensionalized rotation rate) Ta is large. The later work of Bassom & Zhang (1994) has been built upon by Julien & Knobloch (1997, 1999) who derive scaled equations in the limit of rapid rotation and explore the vertical structure of the flow, the heat transport through the layer, and three-dimensional pattern selection near onset.

In this paper we examine composite limits of rapid rotation and small Prandtl number. It is well known that when the Prandtl number $\sigma < 0.677$ and the Taylor number exceeds a critical value $Ta_c(\sigma)$, which depends on whether rigid or stress-free vertical boundary conditions are employed, the onset of convection in an infinite plane layer is oscillatory. As σ becomes small, though, it is apparent that different scalings to those used when $\sigma \sim 1$ and $Ta \to \infty$ may become important. We examine those scalings here. In particular we show how the results of Zhang & Roberts (1997) and Bassom & Zhang (1998) complement those of Julien & Knobloch (1999), and find an intermediate scaling which explains the behaviour of stability boundaries seen in a study of pattern selection at finite Taylor number by Dawes (2000). Physically the leading-order equations describe the balance between the fast oscillation of the convection and rotation: a linear balance leading to a linear momentum equation at leading order if the horizontal structure of the flow is sufficiently simple. This is in sharp contrast to non-rotating low Prandtl number convection where the nonlinear inertial term $\boldsymbol{u} \cdot \nabla \boldsymbol{u}$ balances the pressure term at leading order.

In § 2 we analyse the linear stability results for convection between stress-free boundaries. In these distinguished limits the choice of stress-free or rigid boundaries above and below the layer becomes unimportant; this is shown in § 3 by extending the work of Clune & Knobloch (1993) and Niiler & Bisshopp (1965) to the present case. Section 4 contains the derivation of the scaled equations and shows that the asymptotics indicate three distinct asymptotic regimes. In § 5 the leading-order equations (which are the same for each regime) are solved exactly for fully nonlinear convection, giving analytic expressions for the mean temperature profile and the Nusselt number. Section 6 then concentrates on the most interesting regime and applies modified perturbation theory to determine pattern selection at onset. In § 7 we comment on and extend the similar results obtained by Bassom & Zhang (1998). In § 8 we compare our results with the experiments of Rossby (1969) and Pfotenhauer, Lucas & Donnelly (1984), and with the numerical simulations of Julien, Knobloch & Werne (1998). Conclusions and directions for further work are presented in § 9.

2. Linear theory and scalings

The governing equations for rotating Boussinesq convection are

$$\frac{1}{\sigma}\frac{\mathrm{D}\boldsymbol{u}}{\mathrm{D}t} + E^{-1}\hat{\boldsymbol{z}} \times \boldsymbol{u} = -\nabla p + RT\hat{\boldsymbol{z}} + \nabla^2 \boldsymbol{u}, \tag{2.1}$$

$$\frac{\mathrm{D}T}{\mathrm{D}t} = \nabla^2 T, \tag{2.2}$$

$$\nabla \cdot \boldsymbol{u} = 0, \tag{2.3}$$

for the velocity field $\boldsymbol{u} = (u_x, u_y, u_z)$ and temperature profile T. The equations have been non-dimensionalized with respect to the thermal diffusive timescale d^2/κ. The

dimensionless groups appearing in (2.1) and (2.2) are the Ekman, Rayleigh and Prandtl numbers:

$$E = Ta^{-1/2} = \frac{\nu}{2\Omega d^2}, \qquad R = \frac{\hat{\alpha} g \Delta T d^3}{\nu\kappa}, \qquad \sigma = \frac{\nu}{\kappa}, \tag{2.4}$$

where ΔT is the imposed temperature difference across the layer, Ω is the dimensional rotation rate, d is the layer depth, $\hat{\alpha}$ is the coefficient of volume expansion and ν, κ and g are constants describing the kinematic viscosity and thermal diffusivity of the fluid, and the acceleration due to gravity. In non-dimensional terms the layer occupies the region $0 \leqslant z \leqslant 1$. Solving the linearized versions of (2.1) and (2.2) about the conduction solution $\boldsymbol{u} = 0$, $T = 1 - z$ in conjunction with 'perfect' boundary conditions (fixed temperature and stress-free vertical boundaries at $z = 0,1$ and periodic in the horizontal) we derive analytic expressions for the critical Rayleigh number R_c, frequency ω_c and preferred wavenumber α_c at the onset of oscillatory convection:

$$R_c = \frac{2\sigma^2\pi^2 Ta}{\alpha_c^2(\sigma+1)} + \frac{2(\pi^2+\alpha_c^2)^3(\sigma+1)}{\alpha_c^2},$$

$$\omega_c^2 = (\pi^2+\alpha_c^2)^2\left[-\sigma^2 + \frac{\sigma^2(1-\sigma)\pi^2 Ta}{(\sigma+1)(\pi^2+\alpha_c^2)^3}\right],$$

$$(\pi^2+\alpha_c^2)^2(\sigma+1)^2(2\alpha_c^2-\pi^2) = \sigma^2\pi^2 Ta. \tag{2.5}$$

This last equation is the result of minimizing R_c over all wavenumbers α_c. If the right-hand side of (2.5) becomes large, so too will the preferred wavenumber of convection. This clearly happens in the limit $Ta \to \infty$ with $\sigma \sim 1$. Here we consider the limit of small σ at the same time by fixing

$$\sigma = sE^{1/n}, \qquad \text{equivalently,} \qquad \sigma^n Ta^{1/2} = s^n, \tag{2.6}$$

with s an $O(1)$ constant, for values of n in the range $1 < n < \infty$. With this scaling, in the limit $E \to 0$ we find the following asymptotic expressions for R_c, ω_c and α_c (using the wavenumber which minimizes R_c):

$$R_c = 3(2s^4\pi^4)^{1/3}E^{4\gamma} \equiv \tilde{R}E^{4\gamma}, \tag{2.7}$$

$$\omega_c^2 = (2s^4\pi^4)^{1/3}E^{4\gamma} \equiv \tilde{\omega}^2 E^{4\gamma}, \tag{2.8}$$

$$\alpha_c = \left(\frac{s^2\pi^2}{2}\right)^{1/6} E^{\gamma} \equiv \tilde{\alpha} E^{\gamma}, \tag{2.9}$$

where

$$-\frac{1}{3} < \gamma \equiv \frac{1}{3}\left(\frac{1}{n} - 1\right) < 0. \tag{2.10}$$

The case $n = 1$ has been partially investigated by Zhang & Roberts (1997) and Bassom & Zhang (1998). We exclude it here (and defer analysis to § 7) because it is clear from equation (2.5) that the critical wavenumber remains $O(1)$ in this limit: it does not become large. Setting $n = \infty$, $\gamma = -1/3$ corresponds to the analysis of Julien & Knobloch (1999); differences between this and the analysis for finite n are highlighted in subsequent sections. Using a poloidal-toroidal decomposition for the velocity field $\boldsymbol{u}$:

$$\boldsymbol{u} = \nabla \times \phi\hat{\boldsymbol{z}} + \nabla \times \nabla \times \psi\hat{\boldsymbol{z}} = \left(\partial_y\phi + \partial_x\partial_z\psi, -\partial_x\phi + \partial_y\partial_z\psi, -\nabla_H^2\psi\right)$$

the governing equations become

$$\frac{1}{\sigma}\partial_t \nabla_H^2 \phi - E^{-1}\partial_z \nabla_H^2 \psi + \frac{1}{\sigma} N_\phi(\phi,\psi) = \nabla^2 \nabla_H^2 \phi, \tag{2.11}$$

$$\frac{1}{\sigma}\partial_t \nabla^2 \nabla_H^2 \psi + E^{-1}\partial_z \nabla_H^2 \phi + \frac{1}{\sigma} N_\psi(\phi,\psi) = \nabla^4 \nabla_H^2 \psi - R\nabla_H^2 T, \tag{2.12}$$

$$\partial_t T + N_T(\phi,\psi,T) = \nabla^2 T, \tag{2.13}$$

where the functions N_i represent the nonlinear terms:

$$N_\phi(\phi,\psi) = (\boldsymbol{\omega}\cdot\nabla)u_z - (\boldsymbol{u}\cdot\nabla)\omega_z, \tag{2.14}$$

$$N_\psi(\phi,\psi) = \hat{\boldsymbol{z}}\cdot\nabla\times\nabla\times(\boldsymbol{\omega}\times\boldsymbol{u}), \tag{2.15}$$

$$N_T(\phi,\psi,T) = \boldsymbol{u}\cdot\nabla T, \tag{2.16}$$

and the horizontal part of the Laplacian $\nabla_H^2 \equiv \partial_{xx}^2 + \partial_{yy}^2$. Complete expressions for these nonlinear terms are given in Appendix A.

3. Boundary conditions in the limit $E \to 0$

In the limit (2.6) the linear stability problem with rigid vertical boundaries becomes identical to that for stress-free boundaries. This strongly suggests, as noted by Clune & Knobloch (1993), that subsequent nonlinear calculations (for example, to determine pattern selection) will yield identical results in the two cases. For this section only we will (for computational convenience) fix the layer to lie in the region $-1/2 \leqslant z \leqslant 1/2$. To analyse the linear stability problem of the trivial solution to (2.11)–(2.13) we write $T = 1/2 - z + \theta$ and derive an evolution equation for θ the departure from the linear temperature profile. We assume the solution *ansatz*

$$\begin{pmatrix} \phi \\ \psi \\ \theta \end{pmatrix} = \begin{pmatrix} \displaystyle\sum_{j=0}^{3} A_j \frac{\sigma T a^{1/2}\lambda_j(\lambda_j^2 - \alpha^2 - \mathrm{i}\omega)}{\alpha^2[\mathrm{i}\omega - \sigma(\lambda_j^2 - \alpha^2)]} \frac{\sinh\lambda_j z}{\cosh\lambda_j/2} \\ \displaystyle\sum_{j=0}^{3} A_j \frac{\alpha^2 + \mathrm{i}\omega - \lambda_j^2}{\alpha^2} \frac{\cosh\lambda_j z}{\cosh\lambda_j/2} \\ \displaystyle\sum_{j=0}^{3} A_j \frac{\cosh\lambda_j z}{\cosh\lambda_j/2} \end{pmatrix} \mathrm{e}^{\mathrm{i}\alpha x + (r+\mathrm{i}\omega)t} \tag{3.1}$$

which satisfies the governing linearized equations. The linearized equations result in a matrix determinant that must vanish for a non-zero solution for the constants A_j to be possible. At marginal stability ($r = 0$) this condition yields a polynomial $P(\lambda) = \sigma^2\lambda^8 + B_3\lambda^6 + B_2\lambda^4 + B_1\lambda^2 + B_0$ which has roots $\pm\lambda_j$, $j = 0,\ldots,3$. The complex coefficients $B_0,\ldots,B_3$ are functions of σ, E, R, α and ω. From these we calculate the asymptotic form of the roots $\pm\lambda_j$ of $P(\lambda)$: only $\pm\lambda_1$ remains finite.

The no-slip boundary conditions

$$\theta = \partial_z\psi = \phi = \psi = 0 \qquad \text{at} \quad z = \pm\tfrac{1}{2} \tag{3.2}$$

provide four linear constraints involving the quantities $\beta_j = \lambda_j \tanh(\lambda_j/2)$. These constraints imply that $\beta_1 \to \infty$ in the limit (2.6), but λ_1 remains finite. Hence λ_1 must tend to a multiple of $\mathrm{i}\pi$ as $E \to 0$, and solving $\beta_1 = \lambda_1 \tanh\lambda_1/2$ for λ_1 (taking the

most unstable mode, corresponding to $\lambda_1 = -\pi^2$) we find

$$\lambda_1 = \mathrm{i}\pi\left(1 + \frac{\mathrm{i}s\sqrt{2}}{\tilde{\omega}}E^{\gamma+1/2}\right) \tag{3.3}$$

so that there is an $O(1)$ contribution from the eigenvalue for the stress-free boundary case, and the other eigenvalues alter the vertical structure only in thin boundary layers near $z = \pm 1/2$. This calculation does not hold in the case $n = 1$, as discussed by Zhang & Roberts (1997): for $n = 1$ the analogous analysis leading to the asymptotic forms of the roots of $P(\lambda)$ shows that as $E \to 0$ two pairs of eigenvalues remain $O(1)$ and the vertical structure does not simplify to the sinusoidal solution for stress-free boundaries, see Appendix B.

What is particularly novel about (3.3) is that the rate of convergence to the asymptotic regime varies greatly with γ. Since $-1/3 < \gamma < 0$, the correction term to λ_1 is between $O(E^{1/6})$ and $O(E^{1/2})$ and the asymptotic regime is reached at larger values of E (smaller values of Ta) when γ is close to zero (n close to 1). However, the scaling analysis of § 4 indicates that the corrections to the leading-order equations are minimized when $n = 4$. In this case the correction term to (3.3) is $O(sE^{1/4}) = O(\sigma)$, indicating a fast rate of convergence to the asymptotic regime when $\sigma \ll 1$.

4. The scaled equations

Using the asymptotic relationships (2.7)–(2.9) we rescale the Rayleigh number R, lengths in the horizontal directions x and y, and time t to select the most unstable modes of convection. Let $R' = E^{-4\gamma}R$, $(x', y') = E^{\gamma}(x, y)$ and $t' = E^{2\gamma}t$, then

$$(\partial_x, \partial_y) = E^{\gamma}(\partial_{x'}, \partial_{y'}), \qquad \partial_t = E^{2\gamma}\partial_{t'}.$$

We expand the temperature profile into horizontally averaged and periodic parts, and also scale ψ, but not ϕ. The choices of scalings come from balancing inertial terms, rotation and the largest nonlinear terms all to appear at leading order:

$$T = \bar{T}(z) + E^{-\gamma}\theta(x, y, z, t), \qquad \psi = E^{-\gamma}\psi'. \tag{4.1}$$

The difference between these scalings and Julien & Knobloch (1999) becomes apparent on substitution into (2.11) and (2.12). Dropping primes, we obtain

$$E^{\gamma-1}\left[\frac{1}{s}\partial_t\nabla_H^2\phi - \partial_z\nabla_H^2\psi - \frac{1}{s}J[\phi, \nabla_H^2\phi]\right] = E^{4\gamma}\nabla_H^4\phi - E^{-1}M_0(\phi, \psi) + O(E^{-\gamma-1}), \tag{4.2}$$

$$E^{2\gamma-1}\left[\frac{1}{s}\partial_t\nabla_H^4\psi + \partial_z\nabla_H^2\phi - \frac{1}{s}\nabla_H^2 J[\phi, \nabla_H^2\psi]\right] = E^{5\gamma}\left[\nabla_H^6\psi - R\nabla_H^2\theta\right] - E^{\gamma-1}M_1(\phi, \psi) + O(E^{-1}), \tag{4.3}$$

where M_0 and M_1 are quadratic nonlinear terms derived from N_ϕ and N_ψ respectively (see Appendix A) and the horizontal Jacobian $J[f, g] \equiv \partial_x f\partial_y g - \partial_y f\partial_x g$. For all values of γ the leading-order terms in the square brackets on the left-hand side of (4.2) and (4.3) remain the same, but as γ varies, the relative importance of the nonlinear terms M_i and the diffusion/buoyancy terms on the right-hand side changes. The temperature equation (2.13) yields a further two equations, at $O(E^{\gamma})$ and (after integration over one period in each horizontal direction and in time, denoted by an overbar) at $O(1)$:

$$\partial_t\theta - \nabla_H^2\psi\partial_z\bar{T} - J[\phi, \theta] = \nabla_H^2\theta, \tag{4.4}$$

n	γ	Ordering	Regime
∞	$-1/3$	$E^{\gamma-1} \sim E^{4\gamma} \gg E^{-1}$	Julien & Knobloch (1999)
$4 < n < \infty$	$-1/3 < \gamma < -1/4$	$E^{\gamma-1} \gg E^{4\gamma} \gg E^{-1}$	I
4	$-1/4$	$E^{\gamma-1} \gg E^{4\gamma} \sim E^{-1}$	II
$1 < n < 4$	$-1/4 < \gamma < 0$	$E^{\gamma-1} \gg E^{-1} \gg E^{4\gamma}$	III
1	0		Bassom & Zhang (1998)

TABLE 1. Regimes giving different subdominant balances in the scaled equations (4.2)–(4.5). Referring to (4.2), the leading-order terms are $O(E^{\gamma-1})$, the next-order nonlinearities are $O(E^{-1})$ and the diffusion term is $O(E^{4\gamma})$. The relative scalings in (4.3) are identical. Note that in the limit $n = 1$ (4.2)–(4.5) are not valid.

$$\partial_{zz}^2 \bar{T} + \partial_z \overline{\left[\theta \nabla_H^2 \psi\right]} = 0. \tag{4.5}$$

These last two equations are valid for all γ. We distinguish three different asymptotic regimes, labelled I, II and III, which are summarized in table 1. In regime I the buoyancy and diffusion terms on the right-hand side of (4.2) and (4.3) are larger than the nonlinear terms M_0 and M_1. In regime II, when $n = 4$ and $\gamma = -1/4$, the diffusive terms exactly balance the nonlinearities although neither set of terms appears at leading order. When $-1/4 < \gamma < 0$ the nonlinearities are larger than the buoyancy/diffusion terms: this is regime III. From these three cases one important qualitative distinction about the dynamics can be drawn immediately. The leading-order terms in (4.2)–(4.5) are invariant under a reflection symmetry which is not present in the equations at finite Ta and σ. This symmetry

$$(\psi, \phi, \theta, \bar{T}) \to (-\psi, -\phi, -\theta, \bar{T}) \tag{4.6}$$

corresponds to a reflection in a vertical plane containing the z-axis, for example $(x, y, z) \to (x, -y, z)$. Physically, the symmetries of rotating convection in the limit (2.6) are the same as those of non-rotating convection. This extra symmetry was noted by Julien & Knobloch (1999) in their analysis, and the same degeneracy is introduced into subsequent weakly nonlinear calculations. The existence of this symmetry has important consequences for the investigation of pattern selection and the stability of solutions. However, as we need to go to higher orders in the perturbation expansion just to derive the critical Rayleigh number for the onset of convection, whether these higher-order terms also have this reflection symmetry is important. The quadratic nonlinearities M_i are the only terms in (4.2)–(4.5) that do not obey the symmetry (4.6): when they are less important than the diffusion/buoyancy terms the degenerate situation persists at next order in E. When they are of equal or greater importance than the diffusive terms the symmetry is broken at next order and the flow distinguishes between co-rotating and counter-rotating perturbations. This is crucial for the analysis of Küppers–Lortz type instabilities of travelling rolls.

In physical terms (4.2) and (4.3) show that the rotational constraint is balanced by the fast oscillation of the convecting flow and the velocity field evolves independently of the temperature field at leading-order. Neither viscous dissipation nor buoyancy play a leading-order role but they appear at the same higher order; this must be the case for viscous forces to influence the critical Rayleigh number for the onset of convection. In this respect the scaled equations are similar to those derived by Bassom & Zhang (1994): the difference is that the nonlinear terms have been vastly simplified.

5. Fully nonlinear solutions at leading order

In this section we investigate fully nonlinear solutions of (4.2)–(4.5). At leading order

$$\frac{1}{s}\partial_t \nabla_H^2 \phi_0 - \partial_z \nabla_H^2 \psi_0 = \frac{1}{s} J[\phi_0, \nabla_H^2 \phi_0], \tag{5.1}$$

$$\frac{1}{s}\partial_t \nabla_H^4 \psi_0 + \partial_z \nabla_H^2 \phi_0 = \frac{1}{s} \nabla_H^2 J[\phi_0, \nabla_H^2 \psi_0], \tag{5.2}$$

$$(\partial_t - \nabla_H^2)\theta_0 - \nabla_H^2 \psi_0 \partial_z \bar{T}_0 = J[\phi_0, \theta_0], \tag{5.3}$$

$$\partial_{zz}^2 \bar{T}_0 + \partial_z \overline{[\theta_0 \nabla_H^2 \psi_0]} = 0, \tag{5.4}$$

where the subscript 0 indicates that $(\phi_0, \psi_0, \theta_0, \bar{T}_0)$ are thought of as the leading-order terms in an expansion in powers of E. These equations are to be solved subject to the boundary conditions $\psi_0 = 0$ at $z = 0, 1$ (impermeability) and $\bar{T}(0) = 1$, $\bar{T}(1) = 0$ (fixed temperatures). We adopt the following *ansatz*:

$$(\psi_0, \phi_0, \theta_0) = (A(z), B(z), C(z))\, h(x, y) \varepsilon^{-\mathrm{i}\omega_0 t} + \text{c.c.} \tag{5.5}$$

where $h(x, y)$ is a function describing the horizontal planform, and c.c. indicates the complex conjugate. Fully nonlinear solutions can be found for any planform which depends only on one horizontal wavenumber, so that $\nabla_H^2 h = -\alpha^2 h$, and in addition satisfies $\partial_x h \partial_y h^* = \partial_x h^* \partial_y h$ (where $*$ denotes complex conjugation). These conditions ensure that the Jacobian terms on the right-hand sides of (5.1)–(5.3) vanish identically, leaving nonlinearities only in the temperature equations. Equations (5.1) and (5.2) have the solution

$$A(z) = \frac{A_0}{\alpha} \sin \pi z, \qquad B(z) = \mathrm{i} A_0 \cos \pi z, \qquad \omega_0 = \frac{\pi s}{\alpha}.$$

A_0 is the undetermined amplitude of convection: at higher orders in the expansion we will determine its evolution on slower timescales. From (5.3) we obtain an expression relating $C(z)$ and $\partial_z \bar{T}_0$. A second relationship is given by integrating equation (5.4) once:

$$\partial_z \bar{T}_0 - \alpha H (C A_0^* + C^* A_0) \sin \pi z = -Nu, \tag{5.6}$$

where the constant Nu is the Nusselt number and $H \equiv \overline{|h|^2}$. These relations together yield

$$Nu = \left(1 + \frac{2H\alpha^4 |A_0|^2}{\alpha^4 + \omega_0^2}\right)^{1/2}, \tag{5.7}$$

$$\bar{T}_0(z) = \int \frac{-(\alpha^4 + \omega_0^2) Nu}{\alpha^4 + \omega_0^2 + 2H\alpha^4 |A_0|^2 \sin^2 \pi z}\, \mathrm{d}z. \tag{5.8}$$

This is a fully nonlinear description of the temperature profile – we have not assumed that the amplitude A_0 is small. Equation (5.8) can be integrated to give a fully nonlinear expression for the mean temperature profile:

$$\bar{T}_0(z) = \begin{cases} 1 - (1/\pi) \tan_P^{-1}(Nu \tan \pi z) & \text{in } 0 \leqslant z < \frac{1}{2} \\ \frac{1}{2} & \text{at } z = \frac{1}{2} \\ -(1/\pi) \tan_P^{-1}(Nu \tan \pi z) & \text{in } \frac{1}{2} < z \leqslant 1, \end{cases} \tag{5.9}$$

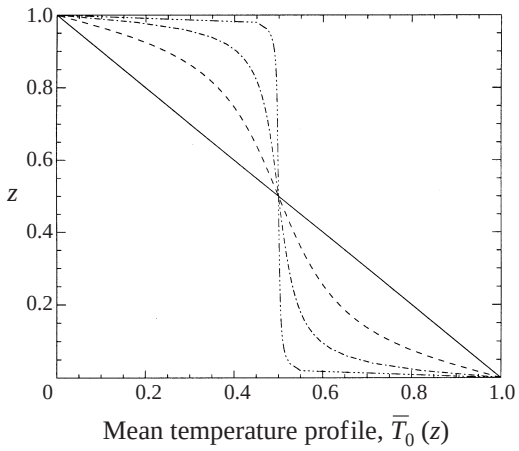

FIGURE 1. The mean temperature profile $\bar{T}_0(z)$ at four values of the Nusselt number Nu: $Nu = 1$ (solid line), $Nu = 3$ (dashed line), $Nu = 10$ (dash-dot line), $Nu = 100$ (dash-dot-dot-dot line).

where $\tan_P^{-1}(x)$ is the principal value of $\tan^{-1}(x)$: $-\pi/2 < \tan_P^{-1} < \pi/2$. Although it is easiest to define the solution for $\bar{T}_0(z)$ piecewise, $\bar{T}_0(z)$ is a smooth function of z, and when $Nu = 1$ (below the onset of convection) we recover the expected linear temperature profile $\bar{T}_0(z) = 1 - z$. Figure 1 shows the variation in $\bar{T}_0(z)$ as Nu increases. The temperature profile becomes uniform throughout the layer and rapid adjustment to satisfy the fixed-temperature boundary conditions occurs in thermal boundary layers near $z = 0, 1$.

Having obtained a fully nonlinear solution at leading order we lack only a relationship between the amplitude of convection A_0 and the (scaled) Rayleigh number R. This can be derived in the most interesting case (regime II, $n = 4$, $\gamma = -1/4$) by expanding the velocity and temperature fields in powers of $E^{1/4}$ and introducing a new timescale $\tau = E^{1/4}t$:

$$(\phi, \psi, \theta, \bar{T}) = (\phi_0, \psi_0, \theta_0, \bar{T}_0) + E^{1/4}(\phi_1, \psi_1, \theta_1, \bar{T}_1) + O(E^{1/2}) \tag{5.10}$$

which gives evolution equations for ϕ_1 and ψ_1 (decoupled from θ_1 and $\bar{T}_1$):

$$\frac{1}{s}\partial_t \nabla_H^2 \phi_1 - \partial_z \nabla_H^2 \psi_1 = -M_0(\phi_0, \psi_0) + \nabla_H^4 \phi_0 - \frac{1}{s}\partial_\tau \nabla_H^2 \phi_0, \tag{5.11}$$

$$\frac{1}{s}\partial_t \nabla_H^4 \psi_1 + \partial_z \nabla_H^2 \phi_1 = -M_1(\phi_0, \psi_0) + \nabla_H^6 \psi_0 - R\nabla_H^2 \theta_0 - \frac{1}{s}\partial_\tau \nabla_H^4 \psi_0. \tag{5.12}$$

A solvability condition is applied by multiplying the right-hand sides by the leading-order solution vector $(\phi_0, \psi_0)^T$ and integrating over one period in the horizontal and in time, and over the whole layer in the z-direction. If the right-hand sides of (5.11)–(5.12) are schematically given by $(F_1, F_2)^T$ then the solvability condition is

$$\mathscr{F}(\phi_0, \psi_0, F_1, F_2) = \int_0^1 \int_0^{2\pi/\alpha} \int_0^{2\pi/\alpha} \int_0^{2\pi/\omega_0} \begin{pmatrix} \phi_0 \\ \psi_0 \end{pmatrix} \cdot \begin{pmatrix} F_1 \\ F_2 \end{pmatrix} \mathrm{d}t\, \mathrm{d}x\, \mathrm{d}y\, \mathrm{d}z = 0. \tag{5.13}$$

There is no resonant contribution from the M_i terms since they contain only quadratic products of ϕ_0 and ψ_0. If A_0 evolves at a frequency ω_1 on the slow timescale τ, i.e. $A_0 = \hat{A}_0 \varepsilon^{-\mathrm{i}\omega_1 \tau}$, the resulting non-resonance condition determines both $|A_0|$ and ω_1:

$$\omega_1 = -s\omega_0, \qquad 2H\alpha^4 |A_0|^2 = R(Nu - 1).$$

Using (5.7) we can eliminate $2H\alpha^4|A_0|^2$ from this expression:

$$Nu = 2\left(\frac{R}{R_c}\right) - 1, \tag{5.14}$$

where $R_c = 2(\alpha^4 + \omega_0^2) = 2(\alpha^6 + s^2\pi^2)/\alpha^2$ is the (scaled) critical Rayleigh number for the onset of convection, agreeing with (2.7)–(2.9). As both R and R_c have been scaled by the same factor of $E^{4\gamma}$ we can replace the scaled R and R_c by the unscaled values in (5.14). The result is a fully nonlinear Nu–R relationship, assuming that our *ansatz* (5.5) holds, independent of the details of the planform. The range of validity of (5.14) can be estimated as $R_c < R < 2^{4/3}R_c$: above $2^{4/3}R_c$ the vertical structure of solutions is likely to contain significant contributions from higher frequency modes $\sin m\pi z$ as these are no longer damped.

We note that the same Nu–R relationship can be derived near onset in regimes I and III and is implicit in the weakly nonlinear analysis of rapidly rotating steady convection by Bassom & Zhang (1994).

6. Weakly nonlinear theory for $n = 4$

From a previous study (Dawes 2000) of pattern selection at finite Ta and σ, two-dimensional travelling rolls $h(x, y) = \mathrm{e}^{\mathrm{i}\alpha x}$ are preferred to three-dimensional planforms close to onset. In this section we compute the stability of a weakly nonlinear travelling roll solution both to all other possible planforms for oscillatory convection on a square lattice, and to roll perturbations at arbitrary angles. Regime II ($n = 4$, $\gamma = -1/4$) is of most interest as not only does it correspond to the subdominant balance between the nonlinear terms M_0 and M_1 and the diffusion/buoyancy terms in (4.2)–(4.5), but the results of Dawes (2000) demonstrate that the stability boundary of travelling rolls to perturbations at $+90^\circ$ to them scales as $\sigma^4 Ta^{1/2} = \text{const}$ in the limit of large Ta. This boundary, and stability boundaries to perturbations at varying angles, can be analysed using a weakly nonlinear expansion in powers of $E^{1/4}$ and ε, the amplitude of convection, assuming that $\varepsilon \ll E^{1/4} \ll 1$. Let

$$(\phi, \psi, \theta) = \sum_{i=0}^{\infty}\sum_{j=1}^{\infty}(\phi_{ij}, \psi_{ij}, \theta_{ij})E^{i/4}\varepsilon^j, \tag{6.1}$$

$$\bar{T}(z) = \bar{T}_0 + \varepsilon\bar{T}_{0,1} + \varepsilon^2\bar{T}_{0,2} + \varepsilon^3\bar{T}_{0,3} + E^{1/4}\varepsilon\bar{T}_{1,1} + \cdots, \tag{6.2}$$

and introduce a set of slow time variables $t_{i,j} = E^{i/4}\varepsilon^j t$ so that

$$\partial_t \to \partial_{t_0} + \varepsilon\partial_{t_{0,1}} + \varepsilon^2\partial_{t_{0,2}} + E^{1/4}\partial_{t_{1,0}} + E^{1/4}\varepsilon\partial_{t_{1,1}} + E^{1/4}\varepsilon^2\partial_{t_{1,2}} + \cdots. \tag{6.3}$$

We now substitute these expansions into the fully nonlinear equations (4.2)–(4.5) and examine terms at each order $E^{i/4}\varepsilon^j$.

6.1. *Solutions at $O(\varepsilon)$ and $O(\varepsilon^2)$*

At first order in the expansion we obtain the linear equations

$$\frac{1}{s}\partial_{t_0}\nabla_H^2\phi_{0,1} - \partial_z\nabla_H^2\psi_{0,1} = 0, \tag{6.4}$$

$$\frac{1}{s}\partial_{t_0}\nabla_H^4\psi_{0,1} + \partial_z\nabla_H^2\phi_{0,1} = 0, \tag{6.5}$$

$$(\partial_{t_0} - \nabla_H^2)\theta_{0,1} + \nabla_H^2\psi_{0,1} = 0, \tag{6.6}$$

where we have used the fact that $\bar{T}_0(z) = 1 - z$ which was deduced from the linearization of (4.5) and the boundary conditions. We first assume the following planform in order to derive amplitude equations to examine the stability of travelling rolls to oscillatory perturbations in the counter-propagating direction (A_2) and at $\pm 90^\circ$ (B_1 and B_2):

$$(\phi_{0,1}, \psi_{0,1}, \theta_{0,1}) = \left(\mathrm{i}\cos \pi z, \frac{\sin \pi z}{\alpha}, \frac{\alpha \sin \pi z}{\alpha^2 - \mathrm{i}\omega_0} \right) h_0(x, y) \mathrm{e}^{-\mathrm{i}\omega_0 t_0} + \text{c.c.}, \tag{6.7}$$

$$h_0(x, y) = A_1 \mathrm{e}^{\mathrm{i}\alpha x} + A_2 \mathrm{e}^{-\mathrm{i}\alpha x} + B_1 \mathrm{e}^{\mathrm{i}\alpha y} + B_2 \mathrm{e}^{-\mathrm{i}\alpha y}. \tag{6.8}$$

We also deduce that $\bar{T}_{0,1}(z) = 0$. This solution to the leading-order problem will be used, as is common in problems of this type, to impose the solvability condition $\mathscr{F}(\phi_{0,1}, \psi_{0,1}, F_1, F_2) = 0$ (5.13) at all further orders in the expansion. The solvability condition does not involve the θ-equation since it decouples from the ϕ and ψ equations at order ε.

At second order in ε imposing the solvability condition implies $\partial_{t_{0,1}} A_1 = 0$ as expected. The equation for the mean temperature indicates that all four modes contribute equally to its deviation from a linear profile and agrees with the fully nonlinear result (5.9):

$$\bar{T}_{0,2}(z) = \frac{-\alpha^4 \sin 2\pi z}{2\pi(\alpha^4 + \omega_0^2)} \left[|A_1|^2 + |A_2|^2 + |B_1|^2 + |B_2|^2 \right]. \tag{6.9}$$

6.2. *Solution at* $O(\varepsilon^3)$

At third order we anticipate that use of the solvability condition will enable deduction of an amplitude equation describing the slow-time evolution of A_1. After applying the solvability condition we obtain a nonlinear evolution equation for A_1:

$$\partial_{t_{0,2}} A_1 = \frac{\mathrm{i}\alpha^4}{4\omega_0} A_1 \left(|B_1|^2 + |B_2|^2 \right). \tag{6.10}$$

This equation, since the coefficient is purely imaginary, describes the nonlinear change (due to B_1 and B_2) in only the phase of A_1, not its modulus. There is no linear term because it would depend on the distance $R - R_c$ above the critical Rayleigh number for the onset of convection, and $R - R_c$ only appears at order $E^{1/4}\varepsilon^3$ in the expansion. There are also no terms $A_1|A_1|^2$ or $A_1|A_2|^2$ since the Jacobian terms vanish for terms which have no dependence on the y coordinate. To obtain an evolution equation involving coefficients which have real parts (from which we can extract stability information) we must proceed to higher orders with the calculation.

6.3. *Solutions at* $O(E^{1/4}\varepsilon)$ *and* $O(E^{1/4}\varepsilon^2)$

We expand the Rayleigh number $R = R_c + \varepsilon^2 R_2 + \cdots$ anticipating that there is no ε term because the amplitude of convection scales as the square root of the distance above onset. We also do not compute higher-order terms in the θ or $\bar{T}$ equations as the solvability condition (5.13) depends only on the ϕ and ψ equation at each order. At $O(E^{1/4}\varepsilon)$, after applying the solvability condition, we obtain expressions for the evolution of A_1 on the timescale $t_{1,0}$ and the critical Rayleigh number R_c:

$$\partial_{t_{1,0}} A_1 = \mathrm{i}s\omega_0 A_1 \quad \text{and} \quad R_c = 2(\alpha^4 + \omega_0^2). \tag{6.11}$$

Hence $A_1 = \hat{A}_1 \mathrm{e}^{-\mathrm{i}\omega_1 t_{1,0}}$ where $\omega_1 = -s\omega_0$ (we drop the carat on $\hat{A}_1$ at higher orders). These results agree with the fully nonlinear analysis of § 5. As the equations at this

order are linear we can, without loss of generality, set $\phi_{1,1} = \psi_{1,1} = 0$ as any non-zero solution could be removed by redefining E.

At $O(E^{1/4}\varepsilon^2)$ the nonlinear terms M_0 and M_1 (given explicitly in Appendix A) enter the equations. From applying the solvability condition we deduce that $\partial_{t_{1,1}} A_1 = 0$.

6.4. *Solution at* $O(E^{1/4}\varepsilon^3)$

Finally we arrive at the order where it is possible to derive a more informative amplitude equation for the evolution of A_1, on the slow timescale $t_{1,2}$. By computing the nonlinear terms at this order and applying the solvability condition we derive equations (related by symmetry) of the form

$$\partial_{t_{1,2}} A_1 = A_1[\mu + a|A_1|^2 + b|A_2|^2 + c|B_1|^2 + d|B_2|^2] + eA_2^* B_1 B_2 \tag{6.12}$$

for the evolution of each of $A_1, \ldots, B_2$; see Knobloch & Silber (1992). The complex coefficients are calculated to be

$$\mu = R_2(\alpha^2 + \mathrm{i}\omega_0), \tag{6.13}$$

$$a = b = -\alpha^4(\alpha^2 + \mathrm{i}\omega_0), \tag{6.14}$$

$$c = -\left[5s^2\pi^2\alpha^2 + 3\alpha^8 + 4\alpha^3\pi^2 - 4\mathrm{i}s\pi\alpha(\alpha^4 + \pi^2)\right](\alpha^2 + \mathrm{i}\omega_0)/4\omega_0^2, \tag{6.15}$$

$$d = -\left[5s^2\pi^2\alpha^2 + 3\alpha^8 - 4\alpha^3\pi^2 - 4\mathrm{i}s\pi\alpha(\alpha^4 - \pi^2)\right](\alpha^2 + \mathrm{i}\omega_0)/4\omega_0^2, \tag{6.16}$$

after rescaling $t_{1,2}$ by a factor of $2(\alpha^4 + \omega_0^2)/s$. The value of e is not needed to determine the stability of travelling rolls. We note first that travelling rolls bifurcate supercritically as $a_r < 0$ for all s (a subscript r denotes the real part of a quantity).

A travelling roll solution $|A_1|^2 = -\mu_r/a_r$ is stable to perturbations in the other three modes if the three quantities

$$(a_r - b_r)/a_r, \qquad (a_r - c_r)/a_r, \qquad (a_r - d_r)/a_r \tag{6.17a–c}$$

are all negative (Knobloch & Silber 1992). As also found by Julien & Knobloch (1999), (6.17*a*) is zero, meaning that the relative stability of travelling rolls and standing rolls $|A_1|^2 = |A_2|^2 = -\mu_r/(a_r + b_r)$ is determined at a yet higher order in the perturbation theory. However, from calculations at finite Taylor number by Dawes (2000), and the discussion in § 7 below, we can assert confidently that travelling rolls are stable with respect to standing rolls. What is not clear is whether travelling rolls are stable to perturbations in the B modes. Figure 2(*a*) shows the variation in (6.17*b*, *c*) with s. When $s < s_{crit} = 2.361$, travelling rolls are unstable to perturbations at $+90°$. The quadratic terms M_0 and M_1 are responsible for the difference in stability to perturbations at $+90°$ and $-90°$ and the corresponding sign differences in the expressions for c and d, (6.15)–(6.16). In the simple limit $Ta \to \infty$ with $\sigma \sim 1$ which was analysed by Julien & Knobloch (1999), the coefficients c and d are forced to be equal at leading order by the 'unwanted' reflection symmetry (4.6).

6.5. *Stability to perturbations at smaller angles*

Since the perturbations to travelling rolls which have the highest growth rate may not be those at 90°, but instead at some smaller angle, the previous analysis can be recast to examine stability to perturbations at any angle $\eta < 90°$. If the planform function $h_0(x, y)$ (6.8) is modified to be

$$h_0(x, y) = A_1 \mathrm{e}^{\mathrm{i}\alpha x} + A_2 \mathrm{e}^{-\mathrm{i}\alpha x} + B_1 \mathrm{e}^{\mathrm{i}\alpha(-x\cos\eta + y\sin\eta)} + B_2 \mathrm{e}^{\mathrm{i}\alpha(x\cos\eta - y\sin\eta)} \tag{6.18}$$

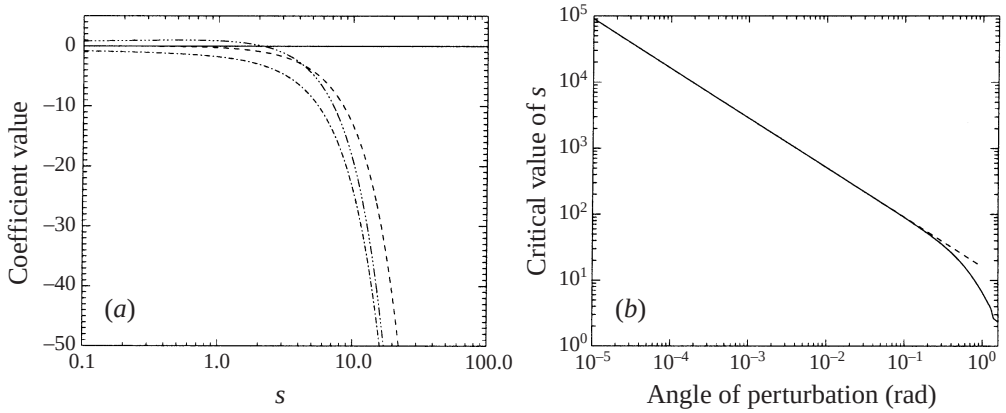

FIGURE 2. (*a*) Variation in coefficients a_r (dashed line), $c_r - a_r$ (dash-dot line) and $d_r - a_r$ (dash-dot-dot-dot line) with s in the case $n = 4$. For $s < 2.361$ travelling rolls are unstable to perturbations at $+90^\circ$ as $d_r - a_r > 0$. (*b*) Value $s_{crit}(\eta)$ below which travelling rolls are unstable to perturbations at an angle η. The dashed line is the asymptotic result $s_{crit} \approx 16.1\eta^{-3/4}$.

the analysis of §§ 6.1–6.4 can be carried out (using MAPLE for example) for arbitrary η. For any fixed η there is a critical value $s_{crit}(\eta)$ below which travelling rolls are unstable to perturbations at an angle η to the original rolls, see figure 2(*b*). Note that $s_{crit}(\eta)$ tends to infinity as $\eta \to 0$ and so at any fixed s, travelling rolls are unstable to perturbations at small enough angles. This agrees with calculations at finite σ and Ta of the growth rates of perturbations at different angles to travelling roll solutions. For small angles it appears that $s_{crit}(\eta) \sim \eta^{-3/4}$ asymptotically. In conclusion, both travelling and standing rolls are unstable near the onset of convection; there are no stable two-dimensional solutions to (5.1)–(5.4).

7. Weakly nonlinear theory for $n = 1$

The scaled equations that were derived in § 4 do not apply in the limit (2.6) corresponding to $n = 1$ since the preferred wavenumber remains $O(1)$ in the limit and the scaling arguments break down. However, this limit is of interest since the transition line between regions of stable travelling and standing rolls asymptotes to a curve of the form $\sigma Ta^{1/2} = \text{const}$ at high Ta (Knobloch & Silber 1990). The weakly nonlinear behaviour in this limit has been partially investigated by Bassom & Zhang (1998) but they were able to deduce only that travelling rolls bifurcate supercritically at onset. In fact, their analysis can be extended to compute the relative stability of travelling and standing rolls, which are *a priori* equally possible candidates for the form of two-dimensional oscillatory convection near onset. The relevant symmetry group of the problem is $O(2)$: the (two-dimensional, i.e. no y-dependence) infinite plane layer is invariant under a circle of translations in the x-direction (due to the imposition of periodicity) and a half-turn rotation about the z-axis which takes $x \to -x$. We propose, at leading order, a solution planform which takes the form of a superposition of travelling rolls with amplitudes A_1 and A_2:

$$(\phi_{0,1}, \psi_{0,1}, \theta_{0,1}) = \left(\mathrm{i}\cos\pi z, \frac{\sin\pi z}{\alpha}, \frac{\alpha\sin\pi z}{\alpha^2 - \mathrm{i}\omega_0}\right) h_0(x)\mathrm{e}^{-\mathrm{i}\omega_0 t_0} + \text{c.c.}, \tag{7.1}$$

$$h_0(x) = A_1\mathrm{e}^{\mathrm{i}\alpha x} + A_2\mathrm{e}^{-\mathrm{i}\alpha x}. \tag{7.2}$$

Following through the modified perturbation expansion we generically derive the normal form for a Hopf bifurcation with $O(2)$ symmetry from the solvability condition at third order:

$$\dot{A}_1 = A_1[\mu + \mathrm{i}\omega + a|A_1|^2 + b|A_2|^2], \tag{7.3}$$

$$\dot{A}_2 = A_2[\mu + \mathrm{i}\omega + a|A_2|^2 + b|A_1|^2]. \tag{7.4}$$

We find that $a_r < 0$ for all s, see figure 3(a). This result was obtained also by Bassom & Zhang (1998) by performing a double expansion similar to that given in § 6. Hence travelling rolls (solutions of the form $|A_1|^2 = -\mu/a_r$, $A_2 = 0$) always bifurcate supercritically. As before, a subscript r denotes the real part of the coefficient. To test the relative stability of travelling and standing rolls it is necessary also to calculate b_r. The calculation of b_r shows, in agreement with Knobloch & Silber (1990), that there is a critical value of s above which travelling rolls are stable and below which standing rolls are preferred. The stability criteria for travelling rolls are plotted in figure 3(a): all stability curves must be negative for stability at a given value of s. When $s < s_c \approx 52.48$, we find $b_r - a_r > 0$ (the dashed curve in figure 3a) which implies travelling rolls are unstable with respect to standing rolls; when $s > s_c$ the inequality is reversed and travelling rolls are stable with respect to standing rolls.

Moreover, as in the case $n = 4$, we can analyse the stability of both travelling and standing rolls to perturbations in the y-directions by including terms for modes B_1 and B_2 in the planform expression (7.2) and working through the perturbation expansion again. The resulting stability theory is given by Knobloch & Silber (1992). It turns out that travelling rolls are always unstable to these y-direction perturbations (the dot-dashed lines in figure 3(a)), and on a faster timescale than that associated with the eigenvalue which determines whether travelling or standing rolls are preferred! The values of c_r and d_r (the real parts of the coefficients of the terms $A_1|B_1|^2$ and $A_1|B_2|^2$ in the A_1 equation) appear at $O(\varepsilon^3)$ in the perturbation expansion where the evolution timescale is $t_{0,2} = \varepsilon^2 t$, but the values of a_r and b_r can only be found by continuing to $O(E\varepsilon^3)$ (as detailed by Bassom & Zhang 1998) where the relevant timescale is $t_{1,2} = E\varepsilon^2 t$. Hence the coefficients a_r and b_r are formally a factor of E smaller than c_r and d_r. To summarize, perturbations in the y-direction are of much greater importance than the relative stability of travelling and standing rolls.

The solid curve in figure 3(b) is always negative, showing that standing rolls also bifurcate supercritically for all s. The enlargement in figure 3(c) shows that over a very small range, $45 < s < 70$, standing rolls are unstable to three-dimensional patterns; for $s > s_c$ the dashed line indicates that standing rolls are also unstable to travelling rolls.

An interesting feature of figure 3(a) is that $c_r = -d_r$ at leading-order. This may be explained by considering the effect of changing $y \to -y$ and $t \to -t$ in the leading-order governing equations for the case $n = 1$ (derived by taking the double curl of the momentum equation (2.1) to eliminate the pressure, writing $\sigma = sE$, and ignoring the higher-order terms which comprise the right-hand side). Equation (2.1) then becomes

$$\partial_t \nabla^2 \boldsymbol{u} + s\partial_z \boldsymbol{\omega} = \nabla \times \nabla \times (\boldsymbol{\omega} \times \boldsymbol{u}). \tag{7.5}$$

The change $(y, t) \to (-y, -t)$ implies that $(\partial_x, \partial_y, \partial_z, u_x, u_y, u_z) \to (\partial_x, -\partial_y, \partial_z, u_x, -u_y, u_z)$ and hence $(\omega_x, \omega_y, \omega_z) \to (-\omega_x, \omega_y, -\omega_z)$. Only the second component of $\boldsymbol{\omega} \times \boldsymbol{u}$ changes sign, hence the second component of the right-hand side changes sign under $(y, t) \to (-y, -t)$. However, the first and third components are the ones which change sign on the left-hand side of (7.5). Hence the transformation $(y, t) \to (-y, -t)$ is equivalent to introducing a minus sign into the nonlinear term on the right-hand side. Consideration of the nonlinear terms at each order in the perturbation expansion

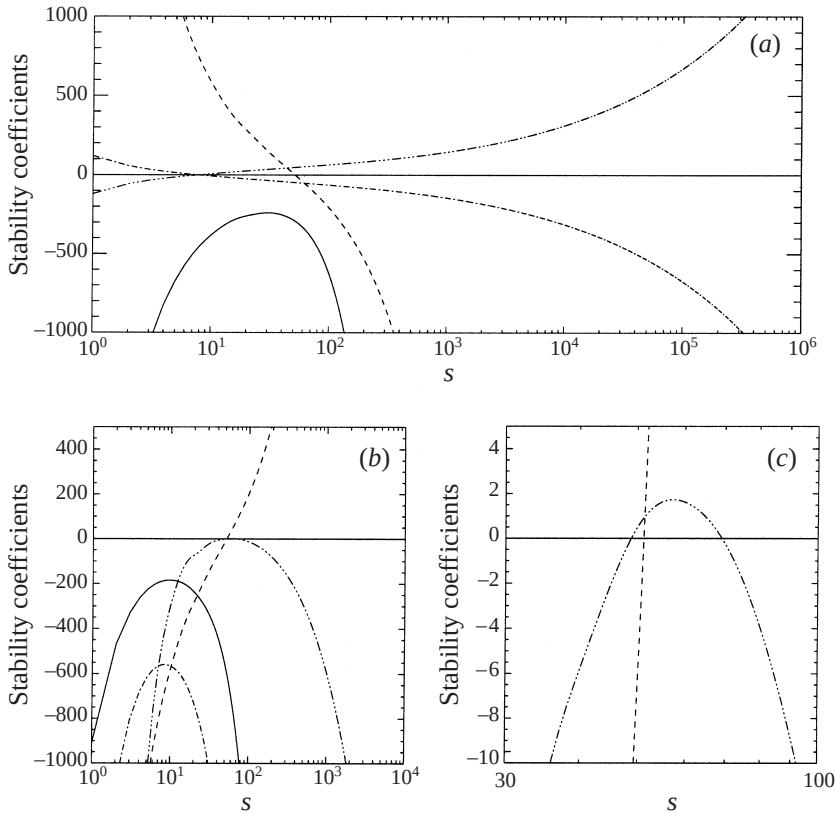

FIGURE 3. (*a*) Stability criteria for travelling rolls in the limit $n = 1$: a_r (solid line) and $b_r - a_r$ (dashed line) are determined at $O(E\varepsilon^3)$, but c_r (dash-dot line) and d_r (dash-dot-dot-dot line) are determined at $O(\varepsilon^3)$. Travelling rolls are stable with respect to standing rolls when $b_r - a_r < 0$. The values of c_r and d_r have been scaled up by a factor of 10 for ease of display. (*b*) Stability criteria for standing rolls using the results of Knobloch & Silber (1992): a_r (solid line), $a_r - b_r$ (dashed line) and $-f_r \equiv c_r + d_r - a_r - b_r$ (dash-dot line) are determined at $O(E\varepsilon^3)$; $|e|^2 - |f|^2$ (dash-dot-dot-dot line) is determined at $O(\varepsilon^3)$. (*c*) Enlargement of (*b*) in the range $30 \leqslant s \leqslant 100$.

shows that changing the sign of the nonlinear term on the right-hand side does not affect either the value of the coefficients c_r and d_r or the evolution equation for A_1 derived at $O(\varepsilon^3)$. However, since this sign change is equivalent to $(y, t) \to (-y, -t)$, the amplitude equation that is derived at third order in ε, analogous to (6.10), must also be invariant under the sign change of y and t. This implies that changing the sign of the time derivative and exchanging B_1 and B_2 leaves the evolution equation unchanged, i.e.

$$\partial_{t_{0,2}} A_1 = A_1[c_r|B_1|^2 + d_r|B_2|^2] = -A_1[c_r|B_2|^2 + d_r|B_1|^2].$$

Invariance implies that $c_r = -d_r$ which is clearly demonstrated by figure 3(*a*). This symmetry is broken by the addition of the diffusion and buoyancy terms at higher orders, but leads to the general conclusion that throughout regime III travelling rolls are never stable to perturbations both at $+90^\circ$ and -90°. This is in contrast to the results for standing rolls which are stable to planforms containing these modes in the $n = 1$ limit when s is low enough, as shown by figure 3(*b*). Further details of the complex dynamics present at finite σ and Ta are given in Dawes (2000).

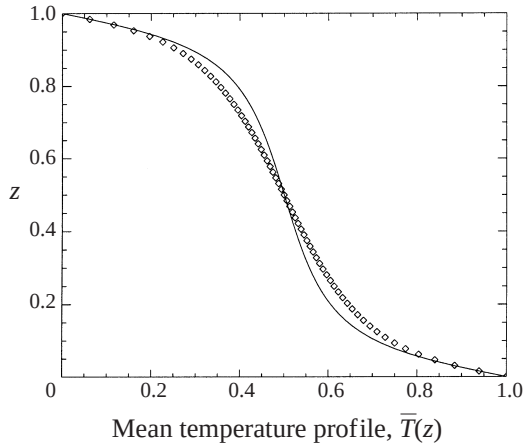

FIGURE 4. Comparison of the time-averaged mean temperature profile from a fully resolved three-dimensional numerical simulation of Julien *et al.* (1998) in the limit of rapid rotation, $n = \infty$. Numerical results at a scaled Rayleigh number $\tilde{R} = 20$ ($\tilde{R}_c = 8.7$) are indicated by $\diamond$. The solid line is the result of (5.9) at the same Nusselt number $Nu = 4.0$.

8. Comparison with experimental work

The preceding analysis shows that three contrasting asymptotic theories dominate different regions of the (σ, Ta)-plane: the limit of rapid rotation only ($n = \infty$), the case $n = 4$, and the case $n = 1$ where the critical wavenumber at onset remains $O(1)$. The leading-order equations (5.1)–(5.4) in the limiting case $n = 4$ are applicable when the parameter s is $O(1)$, say $0.1 \leqslant s \leqslant 10.0$ and the lower-order corrections to (5.1)–(5.4) are negligible. Since these corrections are a factor $E^{1/4}$ smaller, we formally require both $10^{-4} \leqslant s^4 = \sigma^4 Ta^{1/2} \leqslant 10^4$ and $Ta^{1/2} \geqslant 10^4$ (requiring $E^{1/4} \leqslant 0.1$). These conditions yield a range of Ta for a given σ. When $\sigma = 0.025$ this indicates $10^4 \leqslant Ta^{1/2} \leqslant 3 \times 10^{10}$ as an approximate range of Ta within which the $n = 4$ limit is valid. At a given Prandtl number, the dynamics at Taylor numbers outside this range would be better described by the cases $n = \infty$ (Julien & Knobloch 1999) or $n = 1$ (Bassom & Zhang 1998).

After a thorough search of the literature on rotating convection there appear to be only two sets of laboratory experiments which report detailed measurements on a low Prandtl number fluid (mercury): those of Rossby (1969) and Fauve, Laroche & Perrin (1985). Throughout the 1950s and 1960s a number of rotating convection experiments were carried out, but these focused on determination of the critical Rayleigh number for the onset of convection and did not explore behaviour much above onset. Rossby's experiments encompass a range of Taylor numbers $10^3 < Ta < 10^9$ while those of Fauve *et al.* (1985) span only $10^4 < Ta < 10^5$. The small number of Rossby's results which do lie in the range of validity defined above for $n = 4$ show a much slower rise in the Nusselt number with R/R_c than that predicted by (5.14). As his photographs and observations make clear, convection becomes irregularly three-dimensional almost immediately above onset. Fauve *et al.* noted hysteresis in their experimental data and described their results in terms of a codimension-2 pitchfork–Hopf bifurcation. For this description to be valid the rotation rate cannot be assumed to be large, which suggests that this hysteresis phenomenon cannot be captured by an asymptotic theory. There is a clear need for more extensive experimental data at higher rotation rates.

Numerical simulations of convection in the limit of rapid rotation ($n = \infty$) with

$\sigma = 1$ have been carried out by Julien *et al.* (1998). These show convergence to a statistically steady state comprising vortices which extend almost the entire depth of the layer. A comparison with (5.14) of the resulting mean temperature profile obtained numerically for a Nusselt number $Nu = 4.0$ at $R/R_c = 2.3$ (personal communication from Dr K. Julien) is given in figure 4. In the limit of rapid rotation the diffusive terms remain part of the leading-order equations of motion. It seems reasonable that their presence causes the resulting mean temperature profile to be less angular than that suggested by (5.14) at the same Nusselt number.

9. Discussion and conclusions

We have examined rapidly rotating convection at low Prandtl number. By taking distinguished limits and scaling the velocity field, temperature field, length and timescales and physical parameters appropriately we have derived scaled equations which describe the asymptotic dynamics of convection.

The scaled equations are tractable analytically because they contain very few nonlinear terms: moreover the $\boldsymbol{u} \cdot \nabla \boldsymbol{u}$ term does not contribute at all for particular planforms which depend on only one horizontal wavenumber. At leading order the rapid rotation is balanced by the time derivative part of the inertial term. This balance of linear terms leads to oscillatory convection with a fast timescale. The buoyancy term is balanced by diffusion at next order, both these processes evolving on a slower timescale. The dominant nonlinearity comes from the equation for the mean temperature profile. The results of § 3 show that the properties of convection near onset are independent of the imposed vertical boundary conditions. In making the poloidal–toroidal decomposition we have neglected a possible mean flow $(U(z,t), V(z,t), 0)$. This is justified by the fact that in the limit (2.6) there is no consistent scaling which couples the mean flow terms into the leading-order equations.

The relative importance of the diffusive terms and subdominant nonlinearities is important, and we divide the asymptotic behaviour into three regimes of which the most interesting and useful one (the case $n = 4$) is where these subdominant terms balance. A fully nonlinear solution for the vertical structure and heat transport through the layer can be obtained analytically at leading order – this has not been found possible in previous related work.

The two central analytic results of this paper (5.9) and (5.14), formally for fully nonlinear convection, are independent of the parameters $n > 1$ and s which determine the distinguished limit. This independence motivates the claim that they are widely applicable: indeed convection experiments on a wide range of fluids with or without rotation show mean temperature profiles similar to figure 1. Any suitable analytic expression has not, to the best of the author's knowledge, been derived for it previously.

Weakly nonlinear analysis of the scaled equations in the cases $n = 4$ and $n = 1$ confirms the asymptotic behaviour of results on pattern selection at onset at finite Taylor number and Prandtl number. The curve which forms the stability boundary of two-dimensional travelling rolls to perturbations at a fixed angle η scales as $\sigma^4 Ta^{1/2} = \text{const}$ for large Ta, but the constant increases without bound as $\eta \to 0$. From Dawes (2000) we know that standing rolls are unstable to travelling rolls in this regime; within the region of the (σ, Ta)-plane where the limit corresponding to $n = 4$ applies we do not expect two-dimensional solutions to be stable. This is in agreement with experimental results. The relative importance of the subdominant nonlinear terms and the diffusive terms plays a key role in determining the growth rates of Küppers–Lortz type instabilities of travelling rolls.

The case $n = 1$ identifies the transition between Küppers–Lortz unstable travelling rolls and stable standing rolls. This transition was not captured by the analysis of Bassom & Zhang (1998) since they did not compute the full amplitude equations describing the Hopf bifurcation with $O(2)$ symmetry that takes place: they omitted the term $A_1|A_2|^2$ in (7.3) and the evolution equation for A_2 (7.4). Moreover, we have considered the stability of travelling and standing rolls to perturbations in modes at right-angles to them.

Further analytical work on this problem is planned, possibly including investigation of the oscillatory analogue of the work of Cox & Matthews (2000) on small-angle instabilities of steady rolls. Much interest has also been generated in similar scaling arguments applied to thermal convection in a vertical magnetic field (Julien, Knobloch & Tobias 1999; Matthews 1999). It is possible that these ideas could be applied profitably there.

Experiments on rotating convection at low Prandtl number show a plethora of interesting phenomena: effects introduced by lateral boundaries include allowing 'wall-modes' of convective motion which allow convective heat transport at Rayleigh numbers below that predicted from the linear theory for an infinite layer (Goldstein *et al.* 1994) and the spontaneous nucleation of defects at the walls which then break up a pattern of rolls (Hu, Ecke & Ahlers 1997). Encouragingly, the experiments of Pfotenhauer *et al.* (1984) using liquid ^{4}He ($\sigma = 0.49$) indicate that the initial slope of the Nu–R/R_c curve increases rapidly to a value of approximately 2 as the rotation rate increases from zero to $Ta^{1/2} \approx 900$. It is hoped that this theoretical work will contribute to the understanding and interpretation of experimental results: experiments with liquid metals (mercury, liquid sodium or gallium) or cooled gas mixtures (helium, helium–xenon or hydrogen–xenon) are able to access the required parameter ranges and should give further physical insights into this problem.

I have benefited greatly from discussions with Michael Proctor, Alastair Rucklidge and Steve Tobias. I am very grateful to Professor S. Fauve, Dr K. Julien and Professor H. T. Rossby for supplying me with experimental results and answering queries. I would also like to thank two anonymous referees for many comments which have improved the presentation and content of this work. This work was funded by the UK EPSRC.

Appendix A. Nonlinear terms

The full expressions for $N_\phi(\phi,\psi)$, $N_\psi(\phi,\psi)$ and $N_T(\phi,\psi,T)$ are included here for completeness. They are defined by (2.14)–(2.16) in terms of the poloidal and toroidal components ϕ and ψ. We define the horizontal Jacobian $J[f,g] \equiv \partial_x f \partial_y g - \partial_y f \partial_x g$.

$$\begin{aligned} N_\phi(\phi,\psi) = &-J[\phi,\nabla_H^2\phi] - J[\nabla^2\psi,\nabla_H^2\psi] + \nabla_H(\nabla_H^2\phi)\cdot\nabla_H(\partial_z\psi) \\ &-\nabla_H(\partial_z\phi)\cdot\nabla_H(\nabla_H^2\psi) - \nabla_H^2\psi\nabla_H^2(\partial_z\phi) + \nabla_H^2\phi\nabla_H^2(\partial_z\psi), \end{aligned} \tag{A 1}$$

$$\begin{aligned} N_\psi(\phi,\psi) = &-\nabla^2\{J[\phi,\nabla^2\phi] + J[\partial_z\phi,\partial_z\psi] - \nabla_H\phi\cdot\nabla_H(\partial_z\phi) \\ &-\nabla_H(\partial_z\psi)\cdot\nabla_H(\nabla^2\psi)\} - \partial_z\{J[\partial_z\psi,\nabla^2\phi] - J[\phi,\nabla^2\partial_z\psi] \\ &-2J[\partial_z\phi,\nabla^2\psi] + \nabla_H\phi\cdot\nabla_H(\nabla^2\phi) + \nabla_H(\partial_z\psi)\cdot\nabla_H(\nabla^2\partial_z\psi) \\ &+\nabla_H^2\psi\nabla^2(\nabla_H^2\psi) + |\nabla_H(\partial_z\phi)|^2 + |\nabla_H(\nabla^2\psi)|^2 + (\nabla_H^2\phi)^2\}, \end{aligned} \tag{A 2}$$

$$N_T(\phi,\psi,T) = -J[\phi,T] + \nabla_H(\partial_z\psi)\cdot\nabla_H T - \nabla_H^2\psi\partial_z T. \tag{A 3}$$

After the scalings of § 4, different terms in (A 1)–(A 3) appear at different orders in the asymptotic expansion: those contained in the subdominant terms M_0 and M_1 are given below. For convenience, M_0 and M_1 are defined containing factors of $1/s$:

$$M_0(\phi,\psi) = \frac{1}{s}\left[(\nabla_H^2\phi)\nabla_H^2\partial_z\psi - (\nabla_H^2\psi)\nabla_H^2\partial_z\phi + \nabla_H(\nabla_H^2\phi)\cdot\nabla_H(\partial_z\psi) - \nabla_H(\partial_z\phi)\cdot\nabla_H(\nabla_H^2\psi)\right], \tag{A 4}$$

$$M_1(\phi,\psi) = \frac{1}{s}\left[\nabla_H^2(\nabla_H\phi\cdot\nabla_H\partial_z\phi) + \nabla_H^2(\nabla_H(\partial_z\psi)\cdot\nabla_H(\nabla_H^2\psi)) - \partial_z\{(\nabla_H^2\psi)\nabla_H^4\psi + (\nabla_H\phi)\cdot\nabla_H(\nabla_H^2\phi) + |\nabla_H(\nabla_H^2\psi)|^2 + (\nabla_H^2\phi)^2\}\right]. \tag{A 5}$$

Appendix B. Vertical structure in the rigid boundary case

Using the scalings (2.7)–(2.9), the roots of $P(\lambda)$ are found to be

$$\lambda_0^2 = (\tilde{\alpha}^2 + \mathrm{i}\tilde{\omega})E^{2\gamma} + O(1), \tag{B 1}$$

$$\lambda_1^2 = -\frac{\tilde{\omega}^2\tilde{\alpha}^2}{s^2} + O(E^{-2\gamma}), \tag{B 2}$$

$$\lambda_2^2 = \mathrm{i}E^{-1} + O(E^{-1-\gamma}), \tag{B 3}$$

$$\lambda_3^2 = -\mathrm{i}E^{-1} + O(E^{-1-\gamma}). \tag{B 4}$$

The no-slip boundary conditions (3.2) demand that

$$\sum_{j=0}^{3} A_j = \sum_{j=0}^{3} A_j \frac{(\lambda_j^2 - \alpha^2 - \mathrm{i}\omega)\sigma Ta^{1/2}}{\sigma(\lambda_j^2 - \alpha^2) - \mathrm{i}\omega}\beta_j = 0, \tag{B 5}$$

$$\sum_{j=0}^{3} A_j \frac{\alpha^2 + \mathrm{i}\omega - \lambda_j^2}{\alpha^2} = \sum_{j=0}^{3} A_j \frac{\alpha^2 + \mathrm{i}\omega - \lambda_j^2}{\alpha^2}\beta_j = 0, \tag{B 6}$$

where $\beta_j = \lambda_j \tanh\lambda_j/2$. In the limit (2.6) the limiting values of β_0, β_2 and β_3 are easily computed in terms of the λ_j. The limiting value of β_1 is computed from the requirement that the determinant of the 4×4 matrix defined by (B 5) and (B 6) vanish. After substituting the limiting values of β_0, β_2 and β_3 we obtain at leading order:

$$\det\begin{pmatrix} 1 & 1 & 1 & 1 \\ O(1) & -(\tilde{\alpha}^2 + \mathrm{i}\tilde{\omega})E^{2\gamma} & \mathrm{i}E^{-1} & -\mathrm{i}E^{-1} \\ O(E^{\gamma}) & -\beta_1(\tilde{\alpha}^2 + \mathrm{i}\tilde{\omega})E^{2\gamma} & (\mathrm{i}E^{-1})^{3/2} & (-\mathrm{i}E^{-1})^{3/2} \\ O(E^{-\gamma}) & -\mathrm{i}\beta_1(\tilde{\alpha}^2 + \mathrm{i}\tilde{\omega})/\tilde{\omega} & \mathrm{i}^{1/2}E^{-3/2-3\gamma}/s & (-\mathrm{i})^{1/2}E^{-3/2-3\gamma}/s \end{pmatrix} = 0$$

which yields

$$\beta_1 = -\frac{\mathrm{i}\tilde{\omega}\sqrt{2}}{s}E^{-\gamma-1/2} + O(E^{-\gamma})$$

and the result (3.3) follows. In the case $n = 1$ where the critical wavenumber α and the frequency ω are $O(1)$ in the limit (2.6), the roots of $P(\lambda)$ are found to be

$$\lambda_0^2 = \tfrac{1}{2}(\mathrm{i}\omega - \delta^2 + [\delta^4 + 4\pi^2\alpha^2 - \omega^2 + 2\mathrm{i}\omega(\pi^2 - \alpha^2)]^{1/2}) + O(E), \tag{B 7}$$

$$\lambda_1^2 = \tfrac{1}{2}(\mathrm{i}\omega - \delta^2 - [\delta^4 + 4\pi^2\alpha^2 - \omega^2 + 2\mathrm{i}\omega(\pi^2 - \alpha^2)]^{1/2}) + O(E), \tag{B 8}$$

$$\lambda_2^2 = \mathrm{i}\left(\frac{\omega}{s} + s\right) E^{-1} + O(1), \tag{B 9}$$

$$\lambda_3^2 = \mathrm{i}\left(\frac{\omega}{s} - s\right) E^{-1} + O(1), \tag{B 10}$$

where $\delta^2 \equiv \alpha^2 + \pi^2$.

REFERENCES

Bassom, A. P. & Zhang, K. 1994 Strongly nonlinear convection cells in a rapidly rotating fluid layer. *Geophys. Astrophys. Fluid Dyn.* **76**, 223–238.

Bassom, A. P. & Zhang, K. 1998 Finite amplitude thermal inertial waves in a rotating fluid layer. *Geophys. Astrophys. Fluid Dyn.* **87**, 193–214.

Busse, F. H. & Clever, R. M. 1981 An asymptotic model of two-dimensional convection in the limit of low Prandtl number. *J. Fluid Mech.* **102**, 75–83.

Chandrasekhar, S. 1961 *Hydrodynamic and Hydromagnetic Stability*. Oxford University Press.

Clever, R. M. & Busse, F. H. 1981 Low-Prandtl-number convection in a layer heated from below. *J. Fluid Mech.* **102**, 61–74.

Clune, T. & Knobloch, E. 1993 Pattern selection in rotating convection with experimental boundary conditions. *Phys. Rev.* E **47**, 2536–2550.

Cox, S. M. & Matthews, P. C. 2000 Instability of rotating convection. *J. Fluid Mech.* **403**, 153–172.

Dawes, J. H. P. 2000 Pattern selection in oscillatory rotating convection. *Physica* D. **147**, 336–351.

Fauve, S., Laroche, C. & Perrin, B. 1985 Competing instabilities in a rotating layer of mercury heated from below. *Phys. Rev. Lett.* **55**, 208–210.

Goldstein, H. F., Knobloch, E., Mercader I. & Net, M. 1994 Convection in a rotating cylinder. Part 2. Linear theory for low Prandtl numbers. *J. Fluid Mech.* **262**, 293–324.

Hu, Y., Ecke, R. E. & Ahlers, G. 1997 Convection under rotation for Prandtl numbers near 1: linear stability, wave-number selection, and pattern dynamics. *Phys. Rev.* E **55**, 6928–6949.

Jones, C. A., Moore, D. R. & Weiss, N. O. 1976 Axisymmetric convection in a cylinder. *J. Fluid Mech.* **73**, 353–388.

Julien, K. & Knobloch, E. 1997 Fully nonlinear oscillatory convection in a rotating layer. *Phys. Fluids* **9**, 1906–1913.

Julien, K. & Knobloch, E. 1999 Fully nonlinear three-dimensional convection in a rotating layer. *Phys. Fluids* **11**, 1469–1483.

Julien, K., Knobloch, E. & Tobias, S. M. 1999 Strongly nonlinear magnetoconvection in three dimensions. *Physica* D **128**, 105–129.

Julien, K., Knobloch, E. & Werne, J. 1998 A new class of equations for rotationally constrained flows. *Theor. Comput. Fluid Dyn.* **11**, 251–261.

Kek, V. & Müller, U. 1993 Low Prandtl number convection in layers heated from below. *Intl J. Heat Mass Transfer* **36**, 2795–2804.

Knobloch, E. & Silber, M. 1990 Travelling wave convection in a rotating layer. *Geophys. Astrophys. Fluid Dyn.* **51**, 195–209.

Knobloch, E. & Silber, M. 1992 Hopf bifurcation with $\mathbb{Z}_4 \times T^2$ symmetry. *Intl Series Numer. Math.* **104**, 241–252.

Matthews, P. C. 1999 Asymptotic solutions for nonlinear magnetoconvection. *J. Fluid Mech.* **387**, 397–409.

Niiler, P. P. & Bisshopp, F. E. 1965 On the influence of Coriolis force on onset of thermal convection. *J. Fluid Mech.* **22**, 753–761.

Pfotenhauer, J. M., Lucas, P. G. J. & Donnelly, R. J. 1984 Stability and heat transfer of rotating cryogens. Part 2. Effects of rotation on heat-transfer properties of convection in liquid ^{4}He. *J. Fluid Mech.* **145**, 239–252.

Proctor, M. R. E. 1977 Inertial convection at low Prandtl number. *J. Fluid Mech.* **82**, 97–114.

Rossby, H. T. 1969 A study of Bénard convection with and without rotation. *J. Fluid Mech.* **36**, 309–335.

Zhang, K. & Roberts, P. H. 1997 Thermal inertial waves in a rotating fluid layer: exact and asymptotic solutions. *Phys. Fluids* **9**, 1980–1987.